Chapter 3

Functional trialkoxysilane mediated controlled synthesis of fluorescent gold nanoparticles and fluoremetric sensing of dopamine

3.1. Introduction

Dopamine (DA) belongs to the catecholamine family, which is a significant component of the neurotransmitter. It plays a vital role in learning and memory, as well as controlling a variety of motivated behaviours, attention span, and neural plasticity in many ways (Wang et al., 2017). In humans, an oversupply or deficiency of dopamine has consequences, including diseases like poor coordination of movement, a decrease in pleasure experiences, and the beginnings of addiction or memory loss (Vijayaraj et al., 2017). Because of the significant impact on physical well-being, it is crucial to establish efficient and rapid techniques for precisely determining DA content in order to diagnose diseases and track their progression (Tao et al., 2013). The detection of DA has been carried out using a variety of analytical techniques over the last few decades, including high-performance liquid chromatography, electrochemistry, chemiluminescence, immunoassays, as well as colorimetric methods (Shi et al., 2019). Although these methods have some limitations, such as insufficient sensitivity and stability, or the requirement for complex pre-treatment and an expensive device, they are still insufficient for the initial diagnosis and follow-up of DA, as illustrated in the literature (Zhao et al., 2018). In order to overcome these major drawbacks, conventional techniques of DA detection are likely to be limited in their application scope and practicality (He et al., 2018). This limitation must be improved by making significant efforts to develop techniques that are simple to use while still being effective for DA detection with good sensitivity. The use of functional trialkoxysilane has been demonstrated in the controlled synthesis of various noble metal nanoparticles and their multimetallic analogues (Pandey et al., 2012; Pandey et al., 2014e; Pandey et al.,2014d; Pandey et al 2015a Pandey et al., 2021b; Pandey et al., 2005).

It has been established that 3-aminopropyltrimethoxysilane (3-APTMS) capped gold ions are effectively transformed into corresponding nanoparticles in the presence of a wide range of reducing agents including 3-glycidoxypropyltrimethoxysilane (3-GPTMS), cyclohexanone, tetrahydrofuran hydroperoxide, formaldehyde, etc differing in their polarity index, providing functional noble metal nanoparticles useful in a variety of aqueous and non-aqueous solvents. The use of 3-GPTMS and 3-APTMS improves the regulated and quick synthesis of functional noble metal nanoparticles within minutes. The use of 3-APTMS control the micellar behaviour of functional gold nanoparticles, whereas optimum concentration of 3-GPTMS enabled precise control on the size of functional AuNPs with controlled fluorescent activity useful in variety of bioanalytical applications (Pandey et al., 2009; Pandey et al., 2012b; Dalirirad et al., 2020; Rodriguez et al., 2013; Wei, et al., 2019). especially in biomarker sensing. where biomarker levels remain at a lower level relative to healthy individuals (Li et al., 2013 Bassareo and DiChiara, 1999; Farjami et al., 2013; Perry et al., 2009). Therefore, precise sensing of dopamine levels is important for early diagnosis with simple and low-cost point-of-care dopamine sensors that may be a valuable asset for bioanalytical chemists, enabling assistants to patients who have a reduced ability to release this important biomarker by providing a reliable self-monitoring system. Several ways of sensing dopamine have been reported in recent years, including photo-sensitive and using hybrid aptamers (Çakar et al.,2022; Roushani et al., 2022). In addition to that, the biomarker has been very precisely probed through the fluorescence technique (Luo et al., 2022). The fluorescence signal reacts more quickly, with major advantages in real-time biomarker sensing recorded based on fluorescence emission intensity. This has proved an efficient technique for selective sensing of clinically significant

analytes (Yang et al., 2022; Teniou et al., 2022). Such an approach involves the use of gold nanoparticles where the size of the nanoparticle controls the fluorescence emission intensity. Accordingly, the aim of the present work is to use fluorescent gold nanoparticles with controlled nanogeometry in the precise real time selective sensing of dopamine in real samples (CSF). The use of functional trialkoxysilanes enabled control over size (6 nm) of AuNPs making them fluorescent via control over 3-APTMS/3-GPTMS ratio. Fluorescence emission intensity signals recorded from functional trialkoxysilane functionalized fluorescent gold nanoparticles were found to be linearly dependent on the concentration of dopamine. Relatively small AuNPs exhibit a high fluorescence emission intensity, which allows for the measurement of nucleus-targeting compounds with standard sensitivity. Functional trialkoxysilane such as 3-APTMS and 3-GPTMS reacted with the Au^{3+} ions and transformed them into Au^{0} ions, resulting in the formation of red-colored fluorescent gold nanoparticles. The present bioanalytical process has been used in identifying dopamine in real samples of CSF and and compared to that of a recently reported method based on various techniques justifying the advantages of current approach. The results on these lines are reported herein.

3 .2. Experimental section

3. 2.1. Materials and reagent

All materials and reagents were of good analytical quality. 3-Aminopropyletrimethoxy silane (3-APTMS), 3-glycidoxypropyltrimethoxysilane (3- GPTMS), methanol, formaldehyde, dopamine hydrochloride (DA), ethylene glycol, sodium hydroxide (NaOH), Sodium chloride, potassium chloride, magnesium chloride and calcium chloride were purchased from Sigma-

Aldrich and ascorbic acid was purchased from Hi-media and ceribralspinal fluid (CSF) collected from IMS-BHU Varanasi and all the experiments were performed using Phosphate buffer and double distilled water.

3.2.2. 3-APTMS and 3-GPTMS-mediated synthesis of Au-NPs

3-Aminopropyletrimethoxy silane (0.020 M in ethylene glycol) was placed in a 5 mL glass vial, followed by the addition of a methanolic solution of tetrachloroauric acid ($HAuCl_4$) (40 mM), The reaction mixture was stirred on a cyclo vertex mixture for 1 min, followed by the addition of 3-glycidoxypropyletrimethoxysilane (3.8 M in ethylene glycol).The reaction mixture was thoroughly mixed on a cyclo vertex for 2 min followed by incubation in a microwave oven for 10 s and the microwave cycle was repeated four to ten times to yield dark red color AuNPs.

3. 2.3. Quantum yield determination

The fluorescence (FL) quantum yield of the 3-APTMS and 3-GPTMS mediated synthesize AuNPs was determined using quinine sulphate as the reference for the calculation. At a 360 nm excitation wavelength, the quantum yield of the quinine sulfate is 0.54, which is a good value for this compound (Bano et al., 2018). We evaluated the absorbance (below 0.1) and FL emission intensity of the quinine sulfate in 0.1 M H_2SO_4 at 360 nm excitation to determine its UV–visible absorbance and FL emission intensity. Analogous experiments were carried out on synthesized AuNPs under identical conditions, and the quantum yield of the FL was calculated using the equation (eq.1) presented in the supplementary information Table. 3.1.

Sample	Integrated intensity at 360 nm	Absorbance at 360 nm	Quantum Yield (%)
Quinine Sulphate (Reference)	95760	0.06	54
Fluorescent gold nanoparticles	13630	0.03	13

$$Qy = Qy_{ref} \frac{I}{A} \frac{A_{ref}}{I_{ref}} \frac{\eta^2}{\eta_{ref}^2} \quad \text{..... eq.1}$$

Table 3.1. Fluorescence quantum yield determination of functional trialkoxysilane mediated synthesized fluorescent AuNPs with reference to quinine Sulphate at excitation wavelength 360 nm from the equation (1).

3. 2. 4. Sensing of DA using AuNPs

All experiments were carried out in a phosphate buffer solution (0.5 mM, pH 7.1). 5 µL of synthesized gold nanoparticles were added to a phosphate buffer solution of varying DA concentrations (ranging from 0.05 µM to 96 µM), placed in 1 cm quartz cuvette and incubated for 5 minutes before fluorescence spectra were recorded. All the fluorescence spectra were taken with a 5/5 slit width with an excitation of 360 nm. In order to make sure that the results were accurate and that a consistent method was used, all measurements were done three times.

3.2.5. Detection of DA in biological fluid.

Human Cereribrospinal fluid (CSF) was taken from Indian Institute of Medical Sciences (B.H.U.) Varanasi, India, and used right away as Ceribrospinal fluid in the study without any filtering. Various calculated spiked concentrations of DA (ranging from 0.05 μM to 0.2 μM) were added into the 1cm quartz cuvette containing fixed concentrations of CSF along with fluorescent AuNPs, followed by incubation for 5 minutes before fluorescence spectra were recorded (Y et al.,2017; Nishan et al., 2021).

3.2. 6. Instrumentation

The Synthesized fluorescent gold nanoparticles (AuNPs) were analyzed through many spectroscopic and micrographic methods. UV-VIS spectroscopy experiments were performed using a Hitachi U-2900 spectrophotometer. Transmission electron microscopy (TEM) was performed to determine the shape and size by TEM, TECHNAI G^2 20 S-TWIN. The fluorescence emission (FL emission) spectroscopy was performed using a Hitachi F7000 fluorescence spectrophotometer. X-ray photoelectron spectroscopy (XPS) was used to determine the binding energy and chemical composition through XPS, K-alpha Thermo Fisher Scientific. XRD spectra were analyzed by using Rigaku MiniFlex 600. The Edinburgh Instrument produced the time-resolved fluorescence spectra, while the Malvern Nano Zeta Sizer measured the zeta potential.

3. 3. Results and discussion

3.3.1 Microwave assisted 3-APTMS and 3-GPTMS mediated controlled synthesis of fluorescent gold nanoparticle

The use of 3-APTMS and 3-GPTMS has already been demonstrated in controlled conversion of gold cations into AuNPs (Pandey et al., 2021b). During the formation of the nanoparticles, 3-APTMS acts as a lewis acid that helps interactions with all metal cations, serving as a potential stabiliser for many metal nanoparticles. 3-APTMS treated metal cations initiate opening of the epoxide ring of 3-GPTMS, forming covalent linkage with nitrogen of organoamine linked to trialkoxysilane, thus enabling the reduction and stabilization of all noble metal cations with precise control over size of AuNPs via control over 3-APTMS/3-GPTMS ratio within 1 min under microwave exposure of the reaction mixture. It is possible to regulate the reduction process of noble metal cations using this reaction scheme with further control over the process in yielding the formation of bimetallic and trimetallic noble metal nanoparticles. 3-APTMS behaves as a micellar agent and the micellar activity is controlled by varying the concentration of the same, allowing processing of as made nanoparticles in a variety of polar and nonpolar solvents, enabling the use of such functional nanoparticles for many practical applications. In addition to that, under optimum concentrations of 3-APTMS during nanoparticle synthesis, an increase in 3-GPTMS concentration allows a subsequent change in nanogeometry of the as-made noble metal nanoparticles. In the present case, we used 3-GPTMS (3.8M) and 3-APTMS (0.020 M) concentrations to make fluorescent gold nanoparticles (AuNPs). Such an alternation allowed a significant change in the size of the gold nanoparticles as discussed vide infra.

3.3.2. Characterization of synthesized fluorescent AuNPs

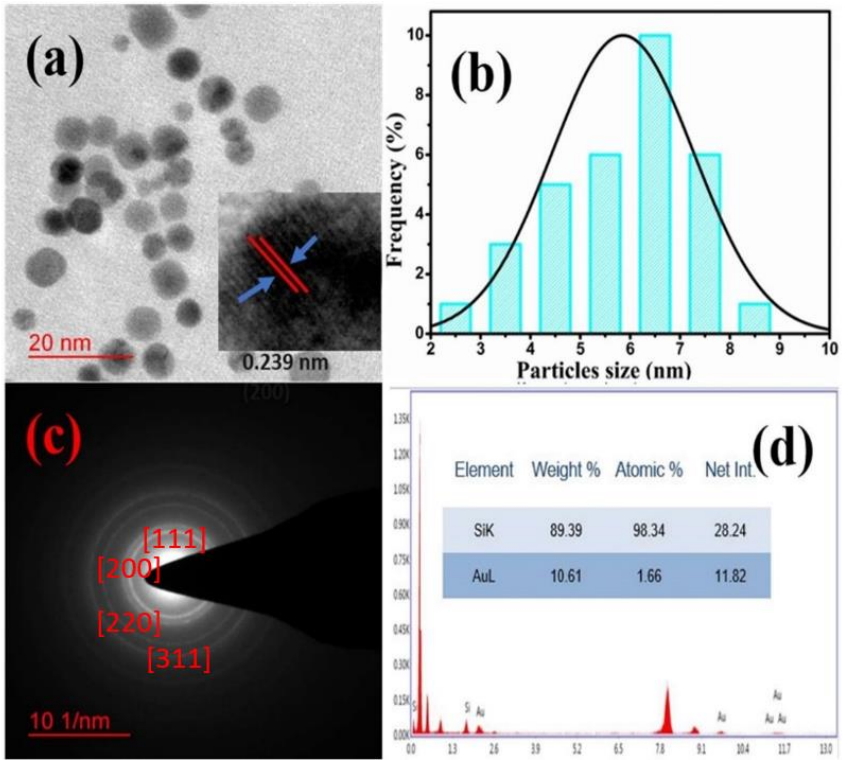

Fig. 3.1 (a) TEM image with the inset showing the fringes of the fluorescent AuNPs (b) particle size distribution histograms were obtained from the TEM image. (c) SAED pattern and (d) EDAX analysis of the fluorescent AuNPs.

The TEM image of the functional trialkoxysilane mediated synthesized fluorescent AuNPs in Fig. 3.1a demonstrates that AuNPs are homogenous in nature and exist in the nanometric range. The inset in Fig. 3.1a demonstrates the crystallinity of AuNPs is found in the face-centered cubic (fcc) structure of Au. The (111) reflection of fcc of Au is represented due to the gap between lattice fringes. Fig. 3.1b, shows the average size of AuNPs ranged from 5.5 to 7.5 nm, with an particles having a size of 6 nm. Fig. 3.1c depicts the SAED pattern of AuNPs, which reveals that the Au nanocrystals were ordered. The EDX of functional

trialkoxysilane mediated synthesized fluorescent AuNPs with a majority of Si and Au is shown in Fig. 3.1d.

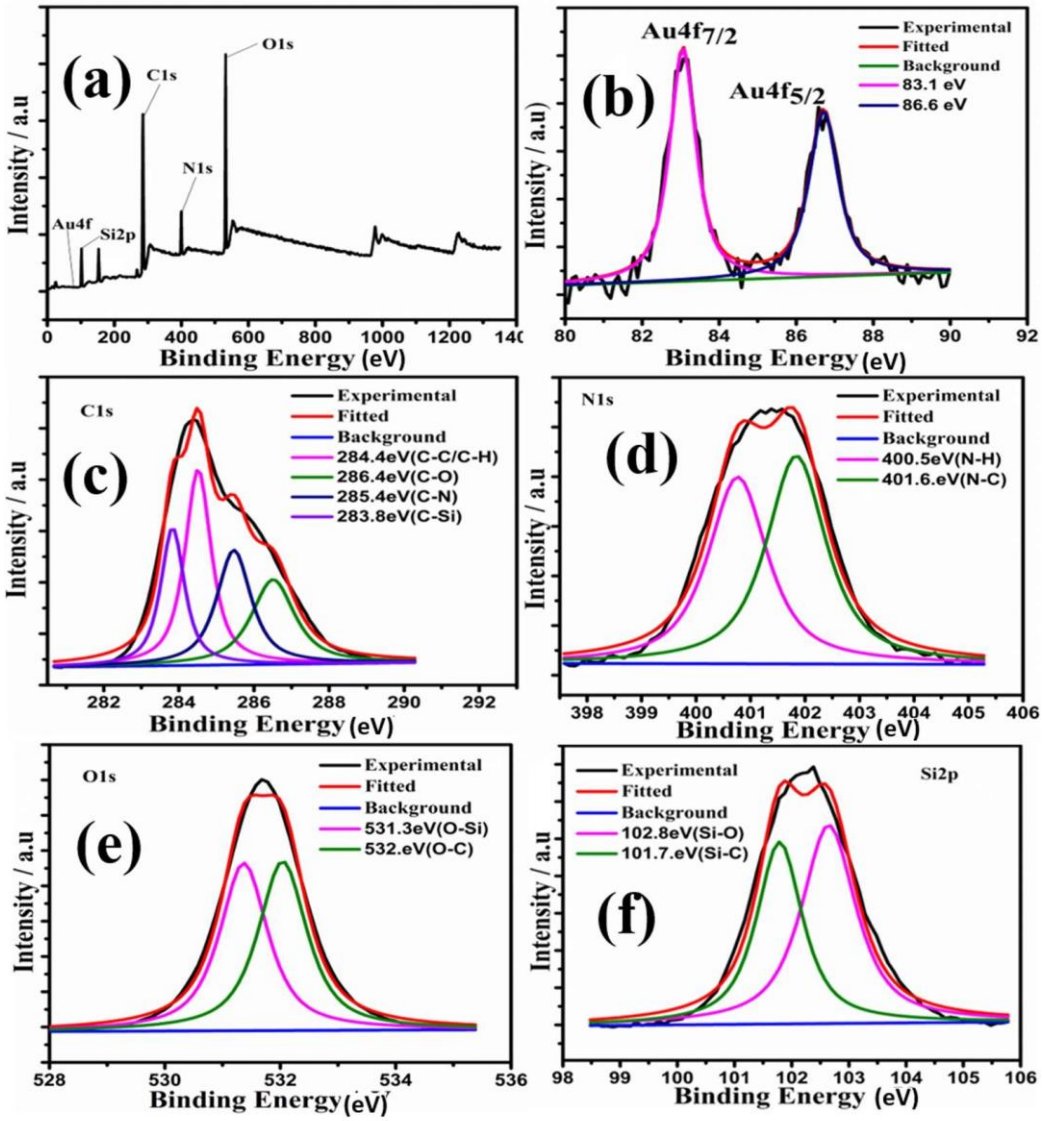

Fig. 3.2 (a) Full scan XPS spectrum (b) Au 4f spectra (c) C1s spectra (d) N1s spectra (e) O1s spectra (f) Si2p spectra of the fluorescent AuNPs.

XPS measurements were made to verify that the constituents in the synthesized materials were properly bonded together. Figure. 2a shows the XPS survey spectrum of C, N, O, Si and Au elements are present in fluorescent AuNPs as predicted. Deconvolution of the associated peaks was done in order to identify the specific binding states shown in Fig. 3.2b to 3.2e. The XPS spectrum of C1s, N1s, O1s, and Si2p are shown in Fig. 3.2b, Fig. 3.2c, Fig. 3.2d, and Fig. 3.2e, respectively. Fig. 3.2b shows the XPS spectrum of Au 4f. X-ray photoelectron spectroscopy was used to detect the oxidation state of gold atoms in AuNPs (Wang et al., 2012). Initially, the oxidation state of gold (Au) atom in $HAuCl_4$ was $Au^{3+,}$ and when 3-APTMS and 3-GPTMS were added to the $HAuCl_4$ solution, the oxidation state of gold (Au) atom was decreased from Au^{3+} to Au^0. Synthesized fluorescent AuNPs were also stabilized with a functional group of 3-APTMS and 3-GPTMS.

The crystallinity and diffracted angles of as-synthesized AuNPs were investigated using XRD from 30 to 90 degrees. Fig. 3.3a, depicts the different two peaks detected for fluorescent AuNPs at 38.4°, 44.6°, 64.6°, 77.7°, and 81.9°, corresponding to (111), (200), (220), (311), and (222) lattice planes, respectively, with the peak at 38.4° being more intense than the other peaks (Nuchprayoon et al., 2018) and XRD analysis of gold nanoparticles confirmed the crystalline nature.. According to HRTEM data, as-prepared functional trialkoxysilane mediated synthesized fluorescent AuNPs were equally dispersed, and Au in the fluorescent AuNPs had the face-centered unit cell (fcc).

The dispersity of functional trialkoxysilane mediated synthesized fluorescent AuNPs was determined by measuring Zeta potentials as shown in Fig. 3.3b. The zeta potential was

measured to be +14 mV, indicating that there is a positive charge over the surface of synthesized fluorescent AuNPs. Because of the greater magnitude of the zeta potential, the AuNPs dispersibility in water over many months and also exhibit remarkable stability of synthesized fluorescent AuNPs.

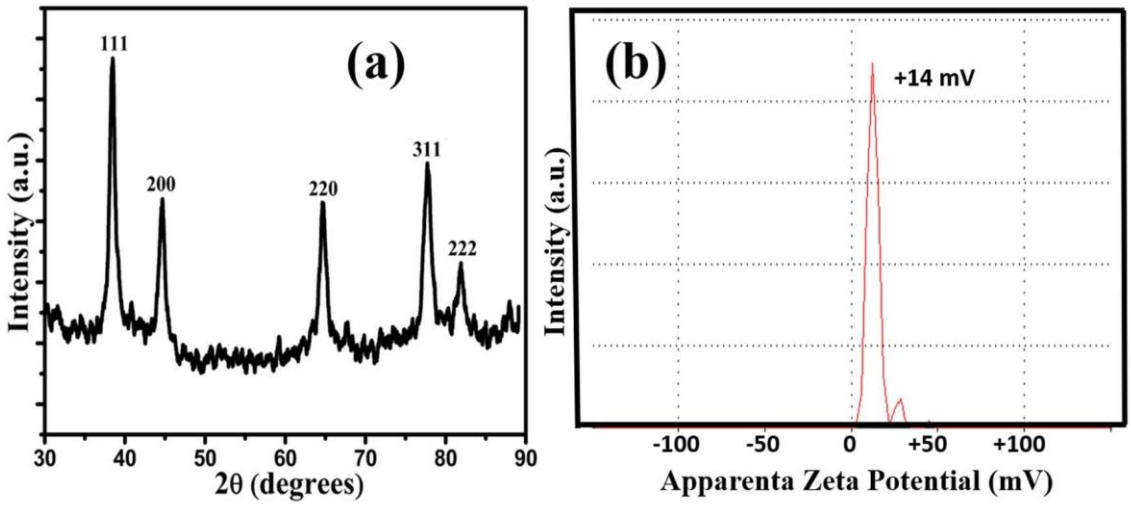

Fig. 3.3 (a) XRD pattern (b) zeta potential of the fluorescent AuNPs.

3.3. 3. Optical characteristics of the fluorescent AuNPs

The fluorescence emission spectra (blue line) and UV-visible (black line) of the fluorescent AuNPs are shown in Fig. 3.4a, ensuring that functionaltrial koxysilane stabilized fluorescent AuNPs emit blue light when exposed to 365 nm UV light in a UV chamber. This finding justify that as made are fluorescent. A single absorption peak appears at 509 nm from the dispersion of AuNPs, while an emission peak appears at 460 nm following excitation at 360 nm. Functional fluorescent AuNPs exhibit excitation-dependent activity in the 290–420 nm range at 10 nm intermissions, as represented in Fig. 3.4b. In the early stages, the

wavelength of the excitation light enhanced from 290 nm to 360 nm the FL emission intensity of the light progressively enhanced with a red shift.

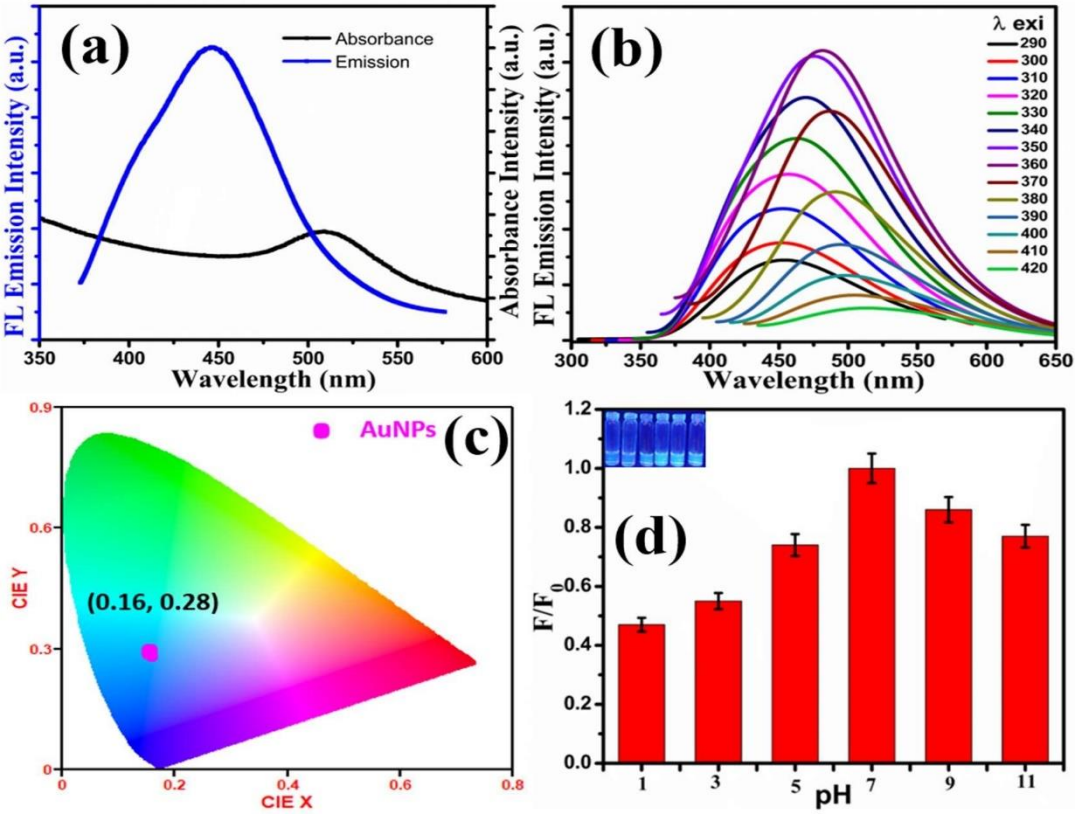

Fig. 3.4 (a) UV-visible absorption spectrum (black line) and fluorescence emission spectrum (blue line). (b) Fluorescence emission spectra showing the different excitation wavelength (290-420nm). (c) Image of CIE coordinates showing the blue color of fluorescent AuNPs. (d) Fluorescence emission intensity at various pH ranging from 1 to 11.

As the experiment progressed, the excitation wavelength increased from 360 nm to 520 nm, and the emission intensity decreased progressively. As a result, our findings show that the excitation-dependent emission pattern observed in as made fluorescent AuNPs is caused by the existence of diverse trap surface states. As made fluorescent AuNPs have

shown remarkable fluorescence quantum yields ~13% when excited at 360 nm with reference to quinine sulfate (54% in 0.1 M H_2SO_4) as a standard. The remarkable quantum yield is due to the nanogeometry and functional activity of AuNPs. Fluorescent AuNPs have established fluorescent nanomaterials for prospective applications in chemical sensing because of their superior photophysical characteristics and high emission quantum yield. Fig. 3.4c, demonstrated the CIE coordination at (0.17, 0.28), which verified the blue FL emission of fluorescent AuNPs. The FL emission intensity of fluorescent AuNPs was investigated at different pH values ranging from 1 to 11 in order to perceive the effect of pH on the FL emission intensity, as demonstrated in Fig. 3.4d. AuNPs were destabilized by the flow of electrons from the functionalities linked to fluorescent AuNPs conduction band (CB) to the acidic medium, resulting in a decrease in their FL intensity. While due to the stability of hydroxide ions in a basic solution, considerable FL intensity was not quenched. However, the maximum FL intensity was reported at neutral pH. As it turns out, the functional trial koxysilane mediated synthesized fluorescent AuNPs was stable at pH levels between 5 and 9. However, for this investigation, a pH of 7.1 was determined to be ideal. The stability of functional fluorescent AuNPs over a range of time intervals has also been studied in the last few months. The functional fluorescent AuNPs exhibited excellent stability at ambient temperature for six months, with no change in their FL intensity, which is shown in Fig. 3.5. justifying that the fluorescent AuNPs have a good ability to sense DA when operated under ideal conditions for prolonged time.

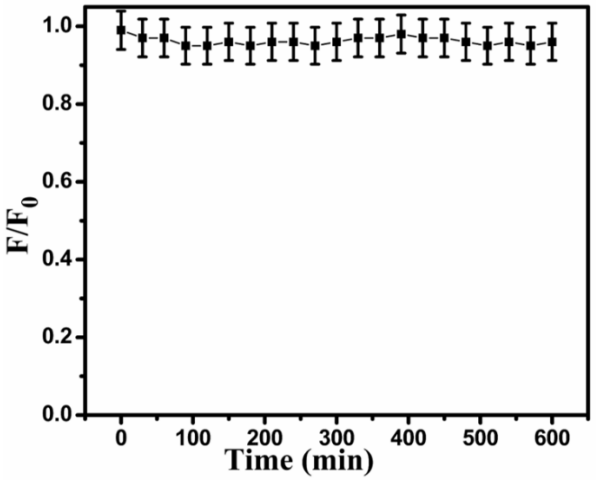

Fig. 3.5**.** Fluorescence emission intensity of fluorescent AuNPs at different time intervals.

3.3.4. DA sensing

After the amounts of DA were raised from 0.05 μM to 96 μM the fluorescence intensity of AuNPs was found to be considerably reduced which is presented in Fig. 3.6a. In this investigation, the fluorescence intensity of AuNPs dropped when the quencher DA was added to the mixture. Fig. 3.6b and inset Fig. 3.6b depicted the relative change in fluorescence intensity vs the intensity at the starting (F_0/F) at 460 nm as a proportion of DA concentration. The Stern-Volmer equation was used to describe the quenching mechanism of fluorescence emission (Thomas et al., 2007). This demonstrates that gold nanoparticles (AuNPs) are a promising and sensitive technique for DA detection. Table 3.2 depicts a comparison of the detection rates of various technique for the detection of dopamine in different environments.

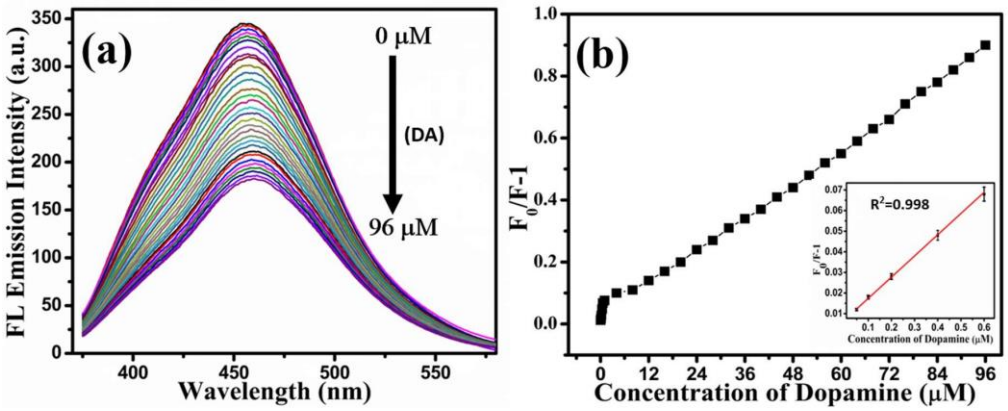

Fig. 3.6 (a) Fluorescence emission intensity decreases with increasing DA concentration from 0 to 96 µM. (b) The linear calibration graph for the concentration range from 0 to 96 µM with inset showing the concentration range from 0 to 0.6 µM.

Materials	Methods	Limit of detection	Reference
Carbon dots based	Fluorescence	5.67 nM	An et al., 2020
Novel lanthanum vanadate-based nanocomposite	Electrochemical	0.046 µM	You et al., 2022
Pyrene -derivatized fluorescence carbon dots	Fluorescence	0.18 µM	Lan et al., 2019
CuFe2O4/Cu9S8/Polly pyrrole ternary nanotube	Colorimetric	1.0 µM	Yang et al.,2017
Cobalt-doped magnetite /graphene nanocomposite	Colorimetric	0.08 µM	Hosseini et al., 2017
Nanoporous AuAg alloy	Electrochemical	0.02 µM	Zhu et al.,2016
Functionaltrialkoxysilane Fluorescent AuNPs	**Fluorescence quenching**	**0.63 nM**	**Present work**

Table 3.2. Comparison performance of various reported methods for DA detection.

3.3.5. Real sample analysis

Real samples (CSF) were used to evaluate the performance of fluorescent AuNPs in CSF for the detection of DA. We added (pH = 7.1) PBS buffer to these real samples CSF and spiked (ranging from 0 μM to 0.2 μM) DA into it. Table 3.3 displays the relative standard deviation and percent recovery for triple measurements of the DA concentration in the real samples.

Sample	Added (μM)	Found ± S. D	% Recovery	RSD (%)
CSF	0.05	0.052 ±0.002	104	3.8
	0.10	0.102 ±0.0003	102	2.9
	0.15	0.148 ± 0.0006	98	4
	0.20	0.201 ± 0.001	101	4.9

Table 3.3. Detection of DA in Spiked CSF.

3.3.6. Selectivity and interference studies

The selectivity experiment seems to be the most important parameter for evaluating the synthesized fluorescent AuNPs sensing efficiency. 5 μL fluorescent AuNPs were added to 1 mL phosphate buffer (0.5 M, pH 7.1) to assess the selectivity of DA detection. We investigated the selective detection of DA in different metal ions and organic compounds, including DA at 96 μM in optimum circumstances. As represented in Fig. 3.7a, DA reduced the fluorescence emission intensity of fluorescent AuNPs compared to other metal ions. To determine the DA selectivity, it was exposed to the UV chamber at excitation wavelength 365 nm.

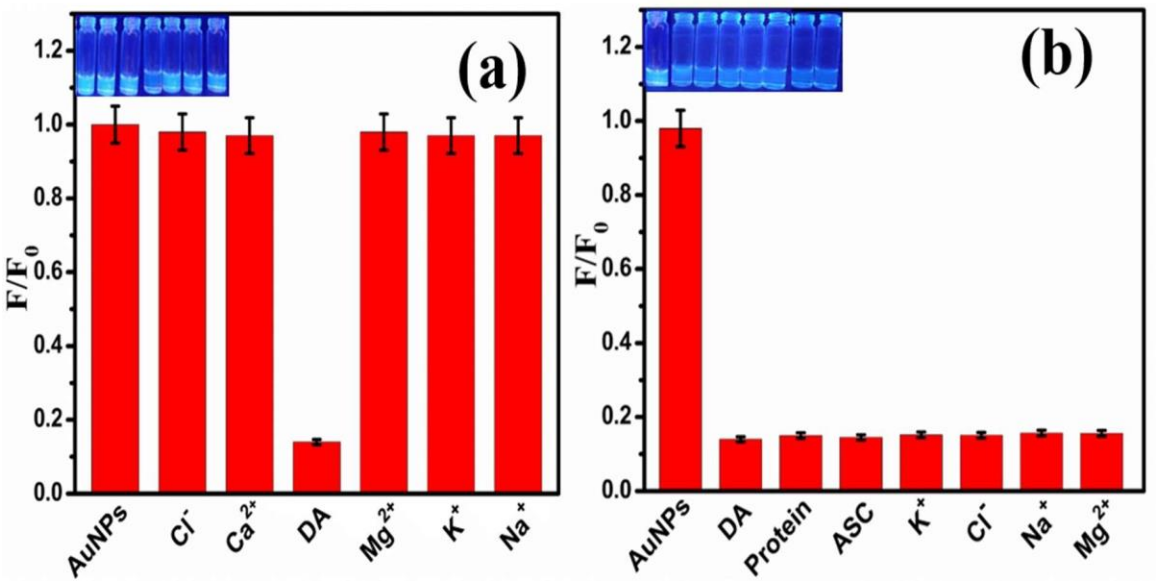

Fig. 3.7 (a) Shows the selectivity of various metal ions and other compounds. (b) interference study of various metal ions and biomolecules in the presence of DA.

The designed sensing system of fluorescent AuNPs with different metal ions and biomolecules in the presence of DA was investigated to understand the interference study of DA. As represented in Fig. 3.7b, there was no noticeable change in the fluorescence emission intensity of AuNPs after the addition of different metal ions and biomolecules. As a consequence, the coexist molecules had almost no influence on the DA detecting system, which was designed particularly to detect DA.

3.3.7. FL Quenching mechanism

As shown in Scheme 3.1, a suitable quenching mechanism of fluorescent AuNPs emission intensity in the addition of dopamine has been proposed. Having two acidic protons in dopamine provides it with excellent ionizable characteristics.

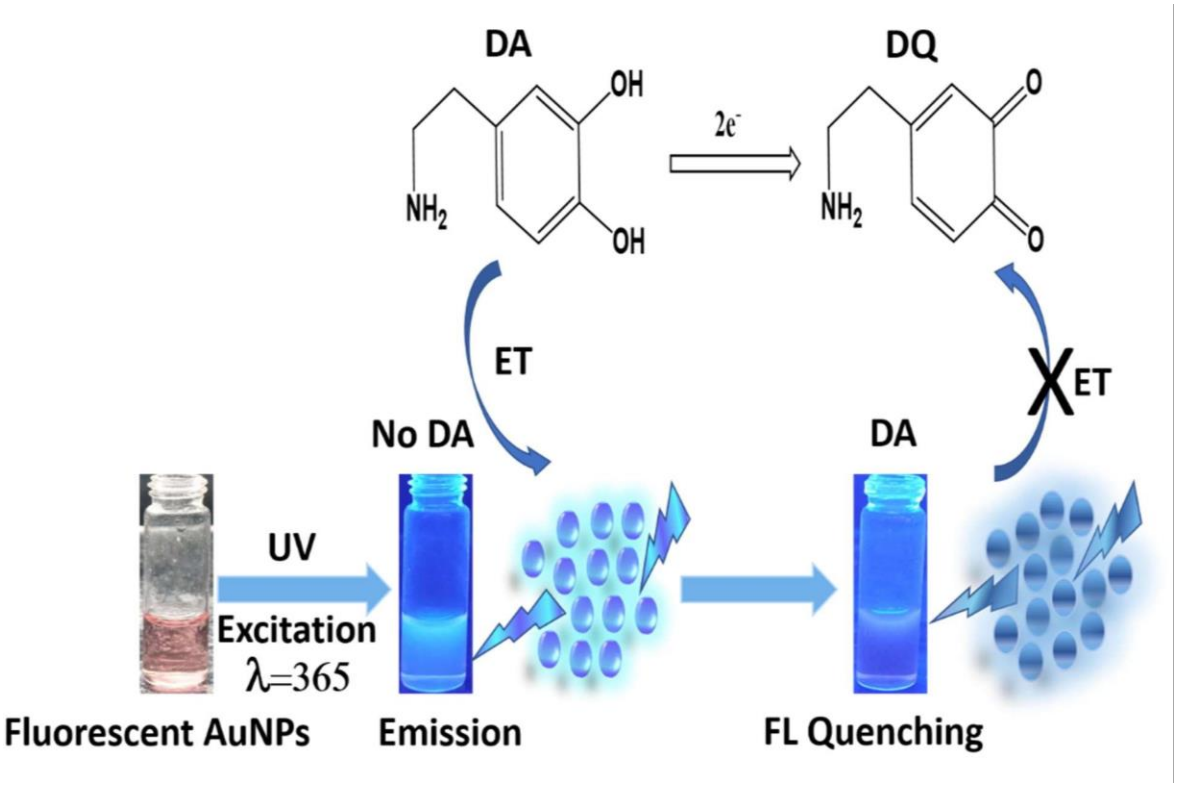

Scheme 3.1. The schematic illustration of fluorescence emission intensity quenching of fluorescent AuNPs with DA and as well as the diagram depicts the reaction mechanism of DA to DQ via electron transfer from DA to fluorescent AuNPs and the donation of those electrons to DQ, which results in fluorescence quenching.

As in the presence of adequate incident radiation (hv), fluorescent AuNPs electrons (e) were accelerated from the valence band (VB) into the conduction band (CB), finally producing an electron-hole pair or exciton. Two acidic protons were removed from dopamine by the energized excitons of AuNPs. Dopamine was likewise prepared to donate these two acidic protons to AuNPs in order to produce DQ through a stable phenoxide-enolate structure. This phenoxide-enolate's aromatic ring resonance structures made it stable. A ring of

dopamine is formed by the delocalization of the negative charge on this oxygen atom of the molecule. The oxygen lone pair interacts with the benzene ring's delocalized electrons. An overlap causes a delocalization that stretches from the ring to an oxygen atom. When those electrons from AuNPs were transferred to DQ, the fluorescence emission intensity of the AuNPs was quenched as a consequence of the electron transfer process (Govindaraju et al., 2017).

3.3.8. Fluorescence Lifetime decay analysis

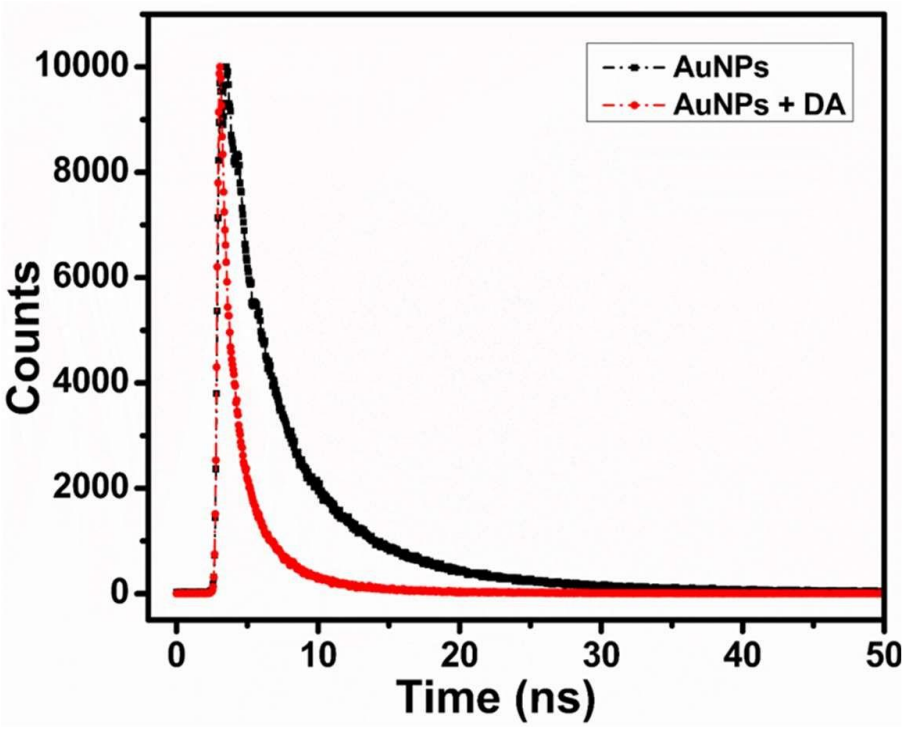

Fig. 3.8. Time resolved fluorescence decay of fluorescent AuNPs in the absence and presence of DA.

As shown in Fig. 3.8, the fluorescence quenching of as produced fluorescent AuNPs in the presence of DA was determined utilising a time resolved fluorescence decay analysis, which was used to determine the quenching. The fluorescence decay over all trajectories can be approximated through a double exponential function, which can be represented by the following formula:

$$D(t) = \sum_{i=1}^{n} ai\ exp\left(-\frac{t}{\tau i}\right)$$

In this equation, D denotes fluorescence decay, τ_i denotes the fluorescence lifetimes of numerous fluorescent forms, and ai denotes the associated pre-exponential factors (Raut et al., 2014). When no acceptor is present, the AuNPs have an average lifetime of 4.25 ns, while the average lifetimes of 1.52 ns were decreased significantly after the adding of electron acceptor DA, indicating that AuNPs transfer electrons to DQ and serve as an electron acceptor to decrease the fluorescence emission intensity of AuNPs through the electron transfer pathway.

3.4. Conclusions

In conclusion, the functional trialkoxysilane-mediated rapid and controlled synthesis of fluorescent AuNPs for the detection of DA in CSF has been established. The functional fluorescent size of AuNPs was determined to be 4-6 nm, which resulted in a quantum yield of 13%, indicating high fluorescence and stability. The structure and properties of fluorescent AuNPs were investigated using a variety of characterization techniques, namely X-ray photoelectron spectroscopy (XPS), photoluminescence spectroscopy (PL), UV-vis

spectroscopy, X-ray diffraction (XRD), and high-resolution transmission microscopy (HRTEM) and Edinburgh Instrument. The synthesized fluorescent AuNPs have a strong binding affinity for DA, resulting in a low limit of detection of 0.63 nM and the ability to detect DA in biological body fluids with high sensitivity and selectivity. This emphasizes the importance of this strategy in developing simple, low-cost, ultra-sensitive detection methods for DA, which might be used for a variety of nanomaterials in the biosensor sector.